Event-triggered Joint Connectivity Topology Containment Control For Unmanned Surface Ship Systems Under Time Delay

Binfeng Tang, Yuge Liu*, and Ying Huang

School of Communication and Signal, Liuzhou Railway Vocational Technical College, Liuzhou 545616, Guangxi. China

Corresponding author. E-mail: tangbf@ltzy.edu.cn

Received: Oct. 19, 2022; Accepted: Dec.16, 2022

For the containment control problem of unmanned surface ship systems (USSs) with time delay and limited communication bandwidth, this paper proposes a distributed event-triggered control strategy using a joint connection switching topology. The communication of unmanned surface ship systems inevitably has delay and the topology is time-varying. Firstly, a joint connectivity switching topology model and the state control method of USSs with delay are designed. Secondly, an event-triggered control mechanism is established, and a new trigger condition of USSs communication is designed. In case of time delay, the USS updates its information and sends it to its neighboring USSs under time delay, minimizes communication consumption and saves energy, and rapidly converges to the steady state. Based on the Lyapunov method, the stability of the system is analyzed, and the Zeno behavior when event-triggered is excluded. It is proved that under the designed control strategy, if the communication topology is jointly connected in a certain time, the follower USS can converge to the convex hull formed by multiple leader USS within a certain delay range. Finally, the correctness and validity of the conclusions are verified by simulation.

Keywords: Unmanned Surface Ship systems (USSs); event-triggered; time delay; jointly connection; switching topology; containment control

http://dx.doi.org/10.6180/jase.202312_26(12).0007

1. Introduction

USS is an important tool for conducting operations at sea, such as environmental monitoring, biological detection, search and rescue, and sensor networks. Therefore, with the development of technology, the motion control of USSs has received considerable attention [1, 2]. The cooperative control of the USSs has been widely used in the military and civil fields, and many scholars have done a lot of related research. The current research has gone beyond the control scope of a single USS, and many works are devoted to the cooperative control of multiple USS. Clearly, cooperative control enables individual USS to perform more challenging tasks, thus increasing efficiency and effectiveness [3, 4]. Cooperative motion control scenarios include coordinated trajectory tracking [5], coordinated target tracking [6] and coordinated target containment [7]. Among them, the coordination target containment system is composed of multiple leaders and multiple followers. Under the corresponding control law, the followers are continuously enveloped in the minimum convex hull enclosed by the leader and complete the specific task.

In recent years, target tracking of maritime ships has been widely studied [8, 9]. In [8], a target tracking controller was developed for a surface ship with random disturbances, which was used to track a target with limited torque under environmental disturbances. Authors proposed a target tracking control law for autonomous surface ships to track a target under the constraints of line of sight and angle in [9].

However, in practice, the follower may not be able to obtain the speed information of the target due to the limited sensing ability. To track leaders whose dynamics are unknown, a variety of control methods can be used [10–12]. Among them, in [12] authors developed a linear target tracking controller for an underactuated unmanned surface vehicle, which was used to track a moving target at high speed. However, the methods proposed in the above work are all target tracking consistency. These methods have somewhat limited the use of the USS in challenging missions, such as using the USS fleet to cooperatively track underwater submarines. Because the follower can only track and control a single target, and the communication topology of the system usually changes due to environmental interference, complete error-free dynamic target tracking cannot be achieved. Therefore, it is of considerable significance and application value to study the containment control problem of unmanned surface ship system with time delay and limited communication bandwidth when it is applied to complete coordination tasks such as sea dangerous goods disposal, enemy search, fire rescue and cooperative transportation.

There have been some research results on the containment control of UAVs, unmanned ground vehicles, and unmanned underwater vehicles [13–16]. Chen et al. [13] proposed a kind of unscented information filter based on weighted average consistency to realize cooperative target tracking. Brinon-Arranz et al. [14] proposed a circular containment formation control method for target tracking of unmanned vehicle fleets. In [15], a local cooperative control method based on output feedback linearization was proposed to solve the problem of moving targets containment control in multi-robot systems subject to nonholonomic constraints, which could realize the speed estimation of moving target and ensure obstacle avoidance between robots. Through the above literature analysis, it can be found that all the proposed control strategies require constant data updates between USS, which requires a large amount of communication and driving resources, which will cause serious waste of communication resources and aggravate the energy. The event-triggered transmission mechanism is that when the gap between the actual state of the system and the set reference state is greater than the set threshold, the neighbor USS communicates with each other and updates the current status. In this way, the communication times of the system are effectively reduced, the occupation of communication resources is reduced, and energy is saved. In the marine environment, the communication bandwidth may be limited, so it is necessary to integrate the event-triggering mechanism into the coordinated target-tracking system to reduce the network burden.

At present, learned most of the literature considers the communication topology as the connected graph is without time delay transmission and communication, the topology structure and communication transmission have intense demand. The reality is because the interaction of information transfer area is limited, many power systems may suffer from some unpredictable structure changes. For example, the repair of random faults and sudden environmental disturbances [17, 18] leads to communication delay at a certain time, disconnection of the topology map, and a possible handover. Therefore, this paper is of important significance for the study of the joint-connected topology containment control of event-triggered unmanned surface ship systems under time delay. This paper analyzes and studies this problem, and its main contributions are as follows:

1. The joint-connected switching topology model is designed, and a state feedback control scheme is designed considering the delay condition. This scheme enables the follower USS to quickly enter the convex hull formed by the leader USS within a certain delay range, to ensure the stability of the system.

2. A new event-triggered control mechanism is designed. With the given event-triggered control condition, the discontinuous communication between USS is established to reduce the update times and energy loss of the controller.

3. Theoretically, the stability of the system is analyzed based on the Lyapunov method, and Zeno behavior triggered by events is excluded. It is proved that if the communication topology is jointly connected in a limited time, the following USS can rapidly converge to the convex hull formed by multiple leading USS agents even if there is a delay.

The remaining parts of this paper are as follows: Section 2 introduces algebraic graph theory and related definition lemma; In Section 3, the control protocol and event-triggered control rules of USSs are designed. In Section 4, the effectiveness of the designed control protocol is proved and the event-triggered Zeno behavior is excluded. In Section 5, the validity of the theoretical results is verified by experimental simulation. Finally, the relevant conclusions are drawn.

Notations: $\boldsymbol{N}$ represents the set of positive integers. $\boldsymbol{R}^n$ represents the vector space on the n-dimensional real body R, $\boldsymbol{R}^{n\times n}$ represents the dimensional real matrix space. diag $\{\boldsymbol{M}_1, \boldsymbol{M}_2, \ldots, \boldsymbol{M}_n\}$ represents the diagonal matrix with elements $\boldsymbol{M}_i, i = 1, 2,$ L, n. $\mathbf{1}_n$ is an n dimensional column vector with all ones. $\mathbf{I}_n$ is an n-dimensional square matrix whose elements on the main diagonal are all ones and the rest are all zeros. $\mathbf{0}$ represents all zero matrices with proper dimension. $\boldsymbol{A} > 0$ denotes A symmetric positive definite matrix, $\rho(\boldsymbol{A})$ denotes the smallest nonzero eigenvalue of matrix A, $\boldsymbol{A}^T$ denotes the transpose of matrix A.

2. Problem description

2.1. Basic knowledge

Suppose that the N th order directed graph $G = \{\boldsymbol{V}, \varepsilon, A\}$ is the information interaction topology among the USSs, where $V = \{1, 2, \mathrm{K}, N\}$ represents the set of vertices of N USSs, and a single agent can be understood as a vertex of the weighted graph $\boldsymbol{G} = \{\boldsymbol{V}, \varepsilon, \boldsymbol{A}\}$. $\boldsymbol{\varepsilon} \in \{\boldsymbol{V} * \boldsymbol{V}\}$ denotes the set of edges formed between the nodes in the graph. $\boldsymbol{A} = \left(a_{ij}\right) \in \boldsymbol{R}^{n\times n}$ denotes the neighbor matrix of graph G, and i, j denotes the corresponding i, j th USS. The neighbors of the ith USS can be denoted by $N_i = \{j \in V : (i, j) \in \varepsilon, i \neq j\}$. Suppose there is no loop of its own nodes in the graph, i.e. $(i, i) \notin \varepsilon$, if $(i, j) \in \varepsilon$, then $a_{ij} > 0$, which means that point j is an adjacent node of point i, otherwise $a_{ij} = 0$. If $(i, j) \in \varepsilon$ and $(j, i) \in \varepsilon$, then the graph G is known as an undirected graph, otherwise it is a directed graph.

The information interaction topology graph G is composed of followers and leaders, which is a disconnected graph under the condition of switching topology. $d_{in}(v_n) = \sum_{i=1}^{n} a_{ij}$ is the in-degree of node i, and define the in-degree matrix of graph G as $D_{in} = \operatorname{diag}\{d_{in}(v_1), \mathrm{L}, d_{in}(v_n)\}$, and the Laplacian matrix as:

$$l_{ij} = \begin{cases} -a_{ij}, i \neq j \\ \sum_{i=1}^{n} a_{ij}, i = j \end{cases} \tag{1}$$

Definition 2.1. [19] Assume the topological graph $G_1, G_2, \ldots, G_\phi$ have the same set of vertices V, and $G_{1-\infty}$ represent the union of the set of edges of $G_1, G_2, \ldots, G_\phi$, and $G_{1-\phi}$ is jointly connected if $G_1, G_2, \ldots, G_\phi$ is connected. ϕ is the number of all possible topologies.

Definition 2.2. [20] Define $\mathbf{Q}$ be the set of real vector space $\boldsymbol{W} \subseteq \mathbf{R}^n$. If there is a point $(1 - c)x + cy \in \boldsymbol{Q}$ for any $c (0 \leq c < 1)$ and any x, y in the set $\mathbf{Q}$, then $\mathbf{Q}$ is convex. The convex hull of point set $Y = \{y_1, y_2, \ldots, y_n\}$ in $\mathbf{W}$ is the smallest convex set containing all points in Y, and expressed by $\mathrm{Co}(Y)$, then

$$\mathrm{Co}(Y) = \left\{ \sum_{i=1}^{n} \beta_i y_i \mid y_i \in Y, \beta_i \in R, \beta_i \geq 0, \sum_{i=1}^{n} \beta_i = 1 \right\}. \tag{2}$$

Definition 2.3. [21] If the control law designed for each follower USS can ensure that they all converge to the convex hull crossed by the dynamic leader USS, then it is said that the USSs with multiple leaders realizes the bounding control, i.e

$$\lim_{t\to\infty} \operatorname{dis}\{xi(t), \operatorname{conv}\{xj(t) \mid i \in F, j \in R\}\} = 0. \tag{3}$$

2.2. The establishment of system model

Consider the USSs composed of $n + m$ USS, including n followers and m leaders. Define the subscript set of the following USS as $F = \{1, 2, \ldots, n\}$, and the subscript set of the leading USS as $R = \{n + 1, n + 2, \ldots, n + m\}$. The system description is as follows:

$$\begin{cases} \dot{x}_i(t) = u_i(t), t \geq 0, \mathrm{i} \in F \\ \mathrm{v}_k(t) \in R, t \geq 0, k \in L \end{cases} \tag{4}$$

where $x_i(t) \in R^n$ and $u_i(t) \in R^m$ represents the state vector of the ith USS and the control input vector, respectively. $\boldsymbol{v}_k(t) \in \mathbf{R}^n$ is the k th state vector leading USS.

Definition 2.4. [21] Consider a set of nonempty, bounded, and continuous time intervals $[t_k, t_{k+1}), k = 0, 1, \ldots n$, where $t_0 = 0, t_{k+1} - t_k \leq T_1, T_1 > 0$. There are finite time subintervals $[t_k, t_{k+1}), k = 0, 1, \ldots$ in time interval $\left[t_k^r, t_k^{r+1}\right), r = 0, 1, \ldots, m_k - 1, t_k^0 = t_k, t_k^{m_k} = t_{k+1}, m_k \geq 0$, that satisfy $t_k^{r+1} - t_k^r \geq T_2, T_2 > 0$

When the communication topology of the USSs switches dynamically, we consider the switching signal ξ_t, when $t \in [0, +\infty), \xi_t \in \aleph, \aleph = \{1, 2, \ldots, \phi\}, G_{\xi_t}$ denotes the topological graph of the USSs at time t, and its Laplacian matrix is denoted by $\mathrm{L}^{\xi^2 t}$.

Definition 2.5. [22] In the USSs, there are m leaders and n followers. Since the leader's input degree is zero and considering the dynamic switching topology of the system, the Laplacian matrix of G can be written as follows:

$$\mathrm{L}^{\xi_t} = \begin{bmatrix} \mathrm{L}_1^{\xi_t} & \mathrm{L}_2^{\xi_t} \\ \mathbf{0} & \mathbf{0} \end{bmatrix} \tag{5}$$

where $\mathrm{L}_1^{\xi_t} \in \mathbf{R}^{n\times n}$ represents the adjacency matrix between the following USS in the corresponding communication topology at time ξ_t.$\mathrm{L}_2^{\xi_t} \in \mathbf{R}^{n\times m}$ represents the adjacency matrix between leading USS in the corresponding communication topology at time ξ_t.

The system meets the following two assumptions:

Assumption 2.1. The information interaction topology graph G_{ξ_t} of USSs switches at time t_k, then its topology structure remains unchanged during span $[t_k, t_{k+1})$. For the followers in the connected subgraph, there exists at least one leader who communicates with the followers.

Assumption 2.2. A communication topology graph G_ξ on a subinterval $\left[t_k^r, t_k^{+1}\right)$ has $\phi \geq 1$ connected subgraphs $G_{\xi t}^i, i = 1, 2, \cdots, \phi$, then there exists a matrix U such that:

$$U_{\xi t}^{T} L_{\xi t} U_{\xi t} = \operatorname{diag}\left\{L_{\xi t}^{1}, L_{\xi t}^{2}, \cdots, L_{\xi t}^{\phi}\right\}, \tag{6}$$

$$e^{T}(t) U_{\xi t} = \left[e_{\xi t}^{1T}(t), e_{\xi t}^{2T}(t), \cdots, e_{\xi t}^{\phi T}(t)\right], \tag{7}$$

$$x^{T}(t) U_{\xi t} = \left[x_{\xi t}^{1T}(t), x_{\xi t}^{2T}(t), \cdots, x_{\xi t}^{\phi}(t)\right] \tag{8}$$

$$x_0^{T} U_{\xi t} = \left[x_0^{1T}, x_0^{2T}, \cdots, x_0^{\phi T}\right], \tag{9}$$

where $x_{\xi t}^{i\,\mathrm{T}}(t) = \left[x_{\xi t_1}^{i}(t), x_{\xi t_2}^{i}(t), \cdots, x_{\xi t_m}^{i}(t)\right], e_{\xi t_t}^{i\,\mathrm{T}}(t) = \left[e_{\xi t_1}^{i}(t), e_{\xi t_2}^{i}(t), \cdots, e_{\xi t_m}^{i}(t)\right], x_0^{i\,\mathrm{T}} = \left[x_{0,1}^{i}, x_{0,2}^{i}, \cdots, x_{0,m}^{i}\right]$

3. System control scheme design

3.1. Design of control law for distributed state observer

The ith control protocol following USS of system Eq. (4) is designed as follows:

$$\begin{aligned} \boldsymbol{u}_i(t) = & \sum_{j \in N_i} -a_{ij}\left(x_i(t-\tau(\mathrm{t})) - x_j(t-\tau(\mathrm{t}))\right) \\ & + \sum_{k=n+1}^{n+m} b_{k,i}\left(v_k(t) - x_i(t-\tau(\mathrm{t}))\right), i \in F, \end{aligned} \tag{10}$$

where $\tau(\mathrm{t})$ is the time delay constant, $b_{k,i}$ is the weighting between the follower USS and the leader USS, if and only if there is a communication connection between them $b_{k,i} > 0$, otherwise $b_{k,i} = 0$

Based on the control protocol (10), the event trigger control rules are combined. $\left\{k_{w_i}^{i}\right\}, i \in F$ is defined as the triggering moment of the i th event following USS, and let $\hat{x}_i(t) = x_i\left(k_{w_i}^{i}\right)$ represent the marking data of the ith event following USS state triggering moment. Protocol (10) can be rewritten as follows:

$$\begin{aligned} \boldsymbol{u}_i(t) = & \sum_{j \in N_i} -a_{ij}\left(\hat{x}_i(t-\tau(\mathrm{t})) - \hat{x}_j(t-\tau(\mathrm{t}))\right) \\ & \sum_{k=n+1}^{n+m} b_{k,i}\left(v_k(t) - \hat{x}_i(t-\tau(\mathrm{t}))\right), i \in F \end{aligned} \tag{11}$$

where $x = (x_1, \ldots, x_n), v = (v_{n+1}, \ldots, v_{n+m})$.Then the dynamic equations of system (11) and control law (12) can be written as follows.

$$\dot{\hat{x}}(t) = (\mathrm{L}_1 \otimes I_n)\, \hat{x}_i\,(t - \tau(\mathrm{t}) + (\mathrm{L}_2 \otimes I_n)\, v \tag{12}$$

4. Design of event triggering rules

Design a distributed event triggering algorithm following USS:

$$\|\Xi\| > \frac{\sigma\rho\left(\mathrm{L}_1\right)}{\|\mathrm{L}_1\|}\|\mathrm{Z}\| \tag{13}$$

where $0 \leq \sigma < 1$, L_1 is the smallest nonzero eigenvalue of $\rho\left(\mathrm{L}_1\right)$, $Z = \operatorname{col}\left(Z_1, \ldots, Z_n\right), \Xi = \operatorname{col}\left(\Xi_1, \ldots, \Xi_n\right)$, when the following USS implementation moves in the convex hull formed by the leader USS, its state is defined as

$$\begin{aligned} \mathrm{Z}_i = & \sum_{j \in N_i} -a_{ij}\left(x_i(t-\tau(\mathrm{t})) - x_j(t-\tau(\mathrm{t}))\right) \\ 1 + & \sum_{k=n+1}^{n+m} b_{k,i}\left(v_k(t) - x_i(t-\tau(\mathrm{t}))\right), i \in F \end{aligned} \tag{14}$$

The state error vector is

$$\begin{aligned} \Xi_i = & \sum_{j \in N_i} -a_{ij}\left(\hat{x}_i(t-\tau(\mathrm{t})) - \hat{x}_j(t-\tau(\mathrm{t}))\right). \\ + & \sum_{k=n+1}^{n+m} b_{k,i}\left(v_k(t) - \hat{x}_i(t-\tau(\mathrm{t}))\right) - \mathrm{Z}_i. \end{aligned} \tag{15}$$

In the designed event-triggering algorithm, when the condition of event-triggering is met, the follower USS updates their information at the trigger time $\left\{k_{w_i}^{i}\right\}$ $i \in F$, and there is no information exchange between USS between the two trigger intervals.

Note 1: The event-triggered condition is determined by the embedded microprocessor installed in the agent, and the event-triggered time is determined by the designed triggered function. When the conditions are met, the event is triggered immediately. The USS transmits the observed value of the current time to the neighbor USS, otherwise, no information is transmitted between the two USS. Compared with the continuous communication between USS or periodic sampling communication, these two methods cause computing burden on the system processor and communication channel blocking due to high communication frequency and a large amount of communication data. The event-triggered mode can effectively reduce the communication times between USS, thus reducing the network communication load and the computation and energy consumption of the controller.

5. Main result

For the convenience of analysis, the following lemma is given:

Lemma 4.1. [19] The topological graph is jointly connected during $[t_k, t_{k+1})$ if and only if

$$\bigcup_{t\in[t,tt+1)} \zeta(\xi_t)=\{1,\ldots,N\} \tag{16}$$

where $\zeta(\xi_t)=\{i \quad : G_{\xi t}\}$ corresponds to all the non-zero eigenvalues of the L_1 matrix $\lambda_i, i\in 1,\ldots,N\}$

Lemma 4.2. [23] Assuming Assumption 2.1 is true, all followers (starting from any initial state) will converge asymptotically into the static convex hull formed by the leader if and only if any of the following conditions are satisfied:

1. $\tau\in(0,\tau_{\min})$ where $\tau_{\min}=\Pi/2\lambda_k, \lambda_k=\lambda_{\max}(L)$
2. The Nyquist graph of $\Gamma(s)=e^{-\tau s}/s$ has a zero envelope around $-1/\lambda_k, \quad \forall k>1$.

In addition, when $\tau=\tau_{\min}$, the system has a globally asymptotically stable frequency vibration solution $\omega=\lambda_k$. The eigenvalues of matrix L can be changed by adding control parameters to the control protocol, and the containment control of the system can be guaranteed according to the actual needs.

Lemma 4.3 [24] Assuming Assumption 2.1 is true, all eigenvalues of L_1 have positive real parts, every entry of $-\mathrm{L}_1^{-1}\mathrm{L}_2$ is nonnegative, and every row of $-\mathrm{L}_1^{-1}\mathrm{L}_2$ has a sum of 1. Let $e(t)=x(t)-\left(\mathrm{L}_1^{-1}\mathrm{L}_2\otimes I_n\right)v$. The system can realize containment control if and only if $\lim_{t\to\infty}e(t)=0$, i.e. $\lim_{t\to\infty}x=\left(-\mathrm{L}^{-1}\mathrm{L}_2\otimes I_n\right)v$.

Lemma 4.4. [25] For any differentiable real function $\omega(t)\in R^n$, there are $n\times n$ dimensional constant matrices $M=M^T>0$ such that the inequality

$$\begin{aligned}&\tau_{\min}^{-1}[\omega(t)-\omega(t-\tau(t))]^{\mathrm{T}}M[\omega(t)-\omega(t-\tau(t))]\\&\le\int_{t-\tau(t)}^{t}\dot\omega^{\mathrm{T}}(s)M\dot\omega(s)ds\end{aligned} \tag{17}$$

holds, where $0\le\tau(t)\le h, t\ge 0$.

Lemma 4.5. [26] For a given symmetric matrix $S=\begin{bmatrix}S_{11} & S_{12}\\ S_{12}{}^T & S_{22}\end{bmatrix}$, where S_{11} and S_{22} are square matrices of the same dimension. S is positive definite if and only if S_{11} and $S_{22}-S_{12}{}^TS_{11}{}^{-1}S_{12}$ are positive definite matrices.

Theorem 4.1 Considering the system (11) in the switched topology, the switched topology described by the switching topology signal F satisfies Assumption 2.1. According to the control laws (11), (13) and Lemma 4.2, for any delay $0<\tau(t)<\tau_{\min}$, the system is stable and all followers can enter the convex hull formed by the leader under any initial condition.

Proof: Choose the Lyapunov function

$$\begin{aligned}V(t)&=e^T(t)e(t)\\&+\int_{t-h}^{t}(s-t+\tau_{\min})\dot e^T(s)\dot e(s)ds\end{aligned} \tag{18}$$

according to Eq. (8) in Assumption 2.2, *V(t)* can be written as

$$\begin{aligned}V(t)&=\sum_{i=1}^{\phi}\left[e_{\xi t}^{iT}(t)e_{\xi t}^{i}(t)\right.\\&\left.+\int_{t-h}^{t}(s-t+\tau_{\min})\dot e_{\xi t}^{iT}(s)\dot e_{\xi t}^{iT}(s)ds\right],\end{aligned} \tag{19}$$

according to (14) and Lemma 4.3,

$$\dot e(t)=-\mathrm{L}_1e(t-\tau(t)), \tag{20}$$

then

$$\begin{aligned}\dot V(t)&=\sum_{i=1}^{\phi}\left\{\left[-\mathrm{L}_{\xi_{\xi t}}^{i}e_{\xi t}^{i}(t-\tau(t))\right]^{\mathrm{T}}e_{\xi t}^{i}(t)\right.\\&+e_{\xi tt}^{iT}(t)\left[-\mathrm{L}_{\xi t}^{i}e_{\xi t}^{i}(t-\tau(t))\right]\\&\left.+\tau_{\min}e_{\xi tt}^{iT}(t)e_{\xi t}^{i}(t)-\int_{t-h}^{t}e_{\xi t}^{iT}(s)e_{\xi tt}^{i}(s)ds\right\}\end{aligned} \tag{21}$$

according to Lemma 4.4, we have

$$\begin{aligned}&-\int_{t-\tau_{\min}^{t}}^{t}e_{\xi t}^{i\,\mathrm{T}}(s)e_{\xi\xi t}^{i}(s)ds\\&\le-\int_{t-\tau(t)}^{t}e_{\xi t}^{i\,\mathrm{T}}(s)e_{\xi tt}^{i}(s)ds\\&\le-\tau_{\min}^{-1}\left[e_{\xi tt}^{i}(t)-e_{\xi tt}^{i}(t-\tau(t))\right]^{\mathrm{T}}\left[e_{\xi tt}^{i}(t)-e_{\xi tt}^{i}(t-\tau(t))\right],\end{aligned} \tag{22}$$

define $y_{\xi t}^{i}(t)=\left[e_{\xi t}^{iT}(t),e_{\xi t}^{iT}(t-\tau(t))\right]^T$, then

$$\begin{aligned}\dot V(t)\le&\sum_{i=1}^{\phi}\left\{-e_{\xi t}^{i\,\mathrm{T}}(t-\tau(t))\mathrm{L}_{1_{\xi t}}^{i\,\mathrm{T}}e_{\xi t}^{i}(t)-e_{\xi t}^{i\,\mathrm{T}}(t)\mathrm{L}_{\xi t}^{i}e_{\xi t}^{i}(t-\tau(t))\right.\\&+\tau_{\min}\left[-\mathrm{L}_{1_{\xi t}}^{i}e_{\xi t}^{i}(t-\tau(t))\right]^{\mathrm{T}}\left[-\mathrm{L}_{1_{\xi t}}^{i}e_{\xi t}^{i}(t-\tau(t))\right]\\&\left.-\tau_{\min}^{-1}\left[e_{\xi t}^{i}(t)-\tilde x_{\xi t}^{i}(t-\tau(t))\right]^{\mathrm{T}}\left[e_{\xi t}^{i}(t)-e_{\xi t}^{i}(t-\tau(t))\right]\right\}\\=&-\sum_{i=1}^{\phi}\tilde y_{\xi t}^{i\,\mathrm{T}}(t)\Phi_{\xi t}^{i}\tilde y_{\xi t}^{i}(t)\end{aligned} \tag{23}$$

where $\Phi_{\xi t}^{i}=\begin{bmatrix}\tau_{\min}{}^{-1}I_m & -\tau_{\min}{}^{-1}I_m+\mathrm{L}_{1_{\xi t}}^{i}\\ -\tau_{\min}{}^{-1}I_m+\mathrm{L}_{1_{\xi t}}^{i} & \\ \tau_{\min}{}^{-1}I_m-\tau_{\min}\mathrm{L}_{1_{\xi t}}{}^{i}\,\mathrm{L}_{\xi t}^{ii} & \end{bmatrix}$

According to Lemma 4.5, $\Phi_{\xi t}^{i}$ is positive definite matrix, $\Phi_{\xi t}^{i}>0$ if and only if $\tau_{\min}^{-1}>0$, where

$$\begin{aligned}\Psi_{\xi t}^{i} &= \left(\tau_{\min}{}^{-1} I_n - \tau_{\min} \mathrm{L}_{1_{\xi t}}^{i\,\mathrm{T}}\, \mathrm{L}_{1_{\xi t}{}^{i}}^{i}\right) \\ &\times \tau_{\min} I_n \times \left(-\tau_{\min}{}^{-1} I_n + \mathrm{L}_{1_{\xi t}}^{i}\right) \\ &= 2\, \mathrm{L}_{1_{\xi t}^{i}}^{i} - 2\tau_{\min} \mathrm{L}_{\xi t^{i}}{}^{\mathrm{T}} \mathrm{L}_{1}{}^{i} t\end{aligned} \tag{24}$$

Obviously, if $2\lambda_g\left(\mathrm{L}_{1_{\xi t}}^{i}\right) - 2\tau_{\min}\lambda_g^2\left(\mathrm{L}_{1_{\xi t}}^{i}\right) > 0, \tau_{\min}{}^{-1} > 0$ and $\Phi_{\xi t}^{i} > 0$, where $\mathrm{L}_{1_{\xi t}}^{i}$ is symmetric, $\mathrm{L}_{1_{\xi t}}^{i}$ is an eigenvalue of $\lambda_g\left(\mathrm{L}_{1_{\xi t}}^{i}\right), g = 1, 2, \cdots, \phi$. If $\lambda_{\mathrm{n}}\left(\mathrm{L}_{1_{\xi t}}^{i}\right) \leq \lambda_{\max}\left(\mathrm{L}_{1_{\xi t}}\right) < \tau_{\min}{}^{-1}, \Psi_{\xi t}^{i} > 0$, according to equation (7) in Assumption 2.2, we have $\lambda_n\left(\mathrm{L}_{1_{\xi t}}^{i}\right) \leq \lambda_{\max}\left(\mathrm{L}_{1_{\xi t}}\right)$, where $\mathrm{L}_{1\xi t}^{i}$ is the largest eigenvalue of $\lambda_{\max}\left(\mathrm{L}_{1_{\xi t}}\right)$. Thus, when Lemma 4.3 is satisfied, $\Phi_{\xi t}^{i}$ is positive definite and $\dot{V}(t) < 0$ ensures the stability of the dynamically switched system.

It has been proved that the system is asymptotically stable. $e(t)$ and $e(t-\tau(t))$ are bounded, according to (20), $\dot{e}(t)$ is bounded. According to equation (7) in Assumption 2.2 and (20), the derivative of $\sum_{i=1}^{i} \tilde{y}_{\xi t}^{i\,\mathrm{T}}(t)\Phi_{\xi t}^{i}\tilde{y}_{\xi t}^{i}(t)$ is bounded. Since $V(t)$ is nonincreasing and has a lower bound of 0, $V(t)$ must have a limit when $t \to \infty$, because

$$\begin{aligned}0 &\geq \int_0^t \left(-\sum_{i=1}^{\phi} \tilde{y}_{\xi t}^{i}(\,\mathrm{s})^{\mathrm{T}} \Phi_{\xi t}^{i} \tilde{f}_{\xi t}^{i}(\,\mathrm{s})\right) ds \\ &\geq \int_0^t \dot{V}(s) ds = V(t) - V(0)\end{aligned} \tag{25}$$

$\int_0^{+\infty}\left(-\sum_{i=1}^{\rho} \tilde{y}_{\xi t}^{i}(\,\mathrm{s})^{\mathrm{T}}\Phi_{\xi t}^{i}\tilde{y}_{\xi t}^{i}(\,\mathrm{s})\right) ds$ exists, $\Phi_{\xi t}^{i} > 0$, thus $\lim_{t\to+\infty}\left(-\sum_{i=1}^{\phi} \tilde{y}_{\xi t}^{i}(t)^{\mathrm{T}}\Phi_{\xi t}^{i}\tilde{y}_{\xi t}^{i}(t)\right) = 0$, $\lim_{t\to+\infty} e_{\xi t}^{i}(t) = 0$, $\lim_{t\to+\infty} x_{\xi t}^{i}(t) = \mathrm{L}_{1\xi t}^{i-1} x_0^{i}$ at any time subinterval $\left[t_k^r, t_k^{r+1}\right), r = 0, 1, \ldots, m_k - 1$, $\lim_{t\to+\infty} x_{\xi t}^{i}(t) = L_{1\xi t}^{i-1} x_0^{i}, i = 1, \cdots, \phi$.

The USSs communication topology is jointly connected in subinterval $[t_k, t_{k+1}), k = 0, 1, \ldots$, $\lim_{t\to+\infty} x_{\xi t}^{i}(t) = L_{1\xi t}^{i}{}^{-1} x_0^{i}, i = 1, \cdots, \phi$ is still true. Since all USS communication topologies in each time interval are jointly connected, from Lemma 4.3, all the following USS states can converge to the convex hull formed by the leading USS, $\lim_{t\to\infty} e(t) = 0$.

Theorem 4.2 According to the control protocol (11) and trigger condition (13), all assumptions and conditions in Theorem 4.1 hold, and for any initial condition, the lower bound of the event trigger interval $\left[k_{w_{i+1}}^{i} - k_{w_i}^{i}\right)$ of system (4) is $\eta > 0$, given by the following equation

$$\begin{aligned}\eta &= \frac{\sigma\rho\left(\mathrm{L}_1\right)}{\|\mathrm{L}_1\|\left(\|\mathrm{L}_1\| + \sigma\rho\left(\mathrm{L}_1\right)\right)} \\ t_{k+1}^{i} &- t_k^{i} \ldots \eta, k \in \{1, 2, \ldots\}.\end{aligned} \tag{26}$$

Proof: According to Eqs. (13) to (15) and Eq. (26)

$$\begin{aligned}&\frac{d\mathrm{P}\Xi\mathrm{P}}{dt\mathrm{P}x\mathrm{P}} \\ &= \frac{\Xi^T x\&}{\mathrm{P}\Xi\mathrm{P}\mathrm{P}x\mathrm{P}} - \frac{x^T x\&}{\mathrm{P}x\mathrm{P}^2} \frac{\mathrm{P}\Xi\mathrm{P}}{\mathrm{P}x\mathrm{P}} \\ &\leq \frac{\mathrm{P}\Xi\mathrm{P}\mathrm{P}x\&\mathrm{P}}{\mathrm{P}\Xi\mathrm{P}\mathrm{P}x\mathrm{P}} + \frac{\mathrm{P}x\&\mathrm{P}\mathrm{P}\Xi\mathrm{P}}{\mathrm{P}x\mathrm{P}\mathrm{P}x\&\mathrm{P}} \\ &= \left(1 + \frac{\mathrm{P}\Xi\mathrm{P}}{\mathrm{P}x\mathrm{P}}\right)\frac{\mathrm{P}x\&\mathrm{P}}{\mathrm{P}x\mathrm{P}} \\ &\leq \left(1 + \frac{\mathrm{P}\Xi\mathrm{P}}{\mathrm{P}x\&\mathrm{P}}\right)\frac{\|\mathrm{L}_1\|\left(\mathrm{P}x\mathrm{P} + \mathrm{P}\Xi\mathrm{P}\right)}{\mathrm{P}x\mathrm{P}} \\ &= \|\mathrm{L}_1\|\left(1 + \frac{\mathrm{P}\Xi\mathrm{P}}{\mathrm{P}x\mathrm{P}}\right)^2\end{aligned} \tag{27}$$

Let $\dot{\theta} = \frac{\|z\|}{\|x\|}, \dot{\theta} \leq \|\mathcal{L}_1\|(1+\theta)^2$, from the above equation that when $\dot{\theta} \leq \|\mathcal{L}_1\|(1+\theta)^2$, the increase rate of θ reaches the maximum.

Let the expression $\theta(t, \theta_0)$ denote the initial value θ_0 and the value at time t. Accordingly, there is H. Let $\theta(\eta, 0)$ be the solution to equality $\theta = \mathrm{P}\mathrm{L}_1\mathrm{P}(1+\theta)^2$.

$$\theta(\eta, 0) = \frac{\eta\mathrm{P}\mathrm{L}_1\mathrm{P}}{1 - \eta\mathrm{P}\mathrm{L}_1\mathrm{P}} \tag{28}$$

In Eq. (28), the growth rate of θ reaches the maximum value. By substituting Eq. (28) into Eq. (13), the shortest event triggering interval η can be obtained:

$$\eta = \frac{\sigma\rho\left(\mathrm{L}_1\right)}{\|\mathrm{L}_1\|\left(\|\mathrm{L}_1\| + \sigma\rho\left(\mathrm{L}_1\right)\right)} \tag{29}$$

So, the lower bound of the event firing interval $\left\{k_{w_{i+1}}^{i} - k_{w_i}^{i}\right\}$ is greater than 0, and the Zeno behavior is excluded.

6. Simulation example

On the basis of theoretical analysis, the correctness of the theory and the effectiveness of the system are verified by a simulation example. The system is composed of 8 USS, as shown in Fig. 1. Nodes 1-5 represent the following USS, and nodes 6-8 represent the leading USS. The initial state following USS is $x_1(0) = (1, -1), x_2(0) = (3, 11), x_3(0) = (5, 20), x_4(0) = (7, -7), x_3(0) = (9, -4)$, The initial state following USS is $x_6(0) = (3, 4), x_7(0) = (7, 6), x_8(0) = (5, 9)$.

As can be seen from Fig. 1, the communication topology of the system is $\{G_1, G_2, G_3\}$, Assume that the topology is switched in the order of $G_1 \to G_2 \to G_3 \to G_1 \to \ldots$, and the topology switching process is shown in Fig. 2. The topology map is switched at a period of 0.9 s. The topology maps in each period form a joint topology of graph $\bar{G}$.

Consider the three jointly connected graphs G1, G2, and G3 in figure 1 , whose union $\bar{G}$ is connected. The Laplacian

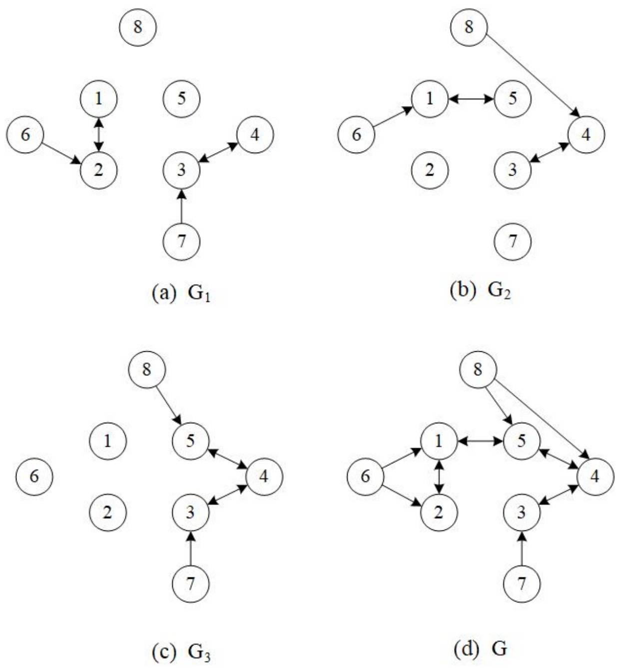

Fig. 1. The communication topology of USSs

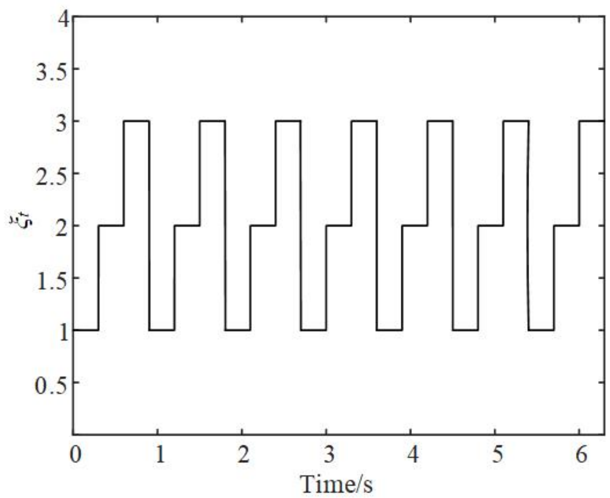

Fig. 2. Process of communication topology switching

matrix $L_1^{\xi_t}, L_2^{\xi,t}$ corresponding to each topology is shown as follows:

$$L_1^1 = \begin{bmatrix} 1 & -1 & 0 & 0 & 0 \\ -1 & 2 & 0 & 0 & 0 \\ 0 & 0 & 2 & -1 & 0 \\ 0 & 0 & -1 & 1 & 0 \\ 0 & 0 & 0 & 0 & 0 \end{bmatrix}$$

$$L_2^1 = \begin{bmatrix} 0 & 0 & 0 \\ -1 & 0 & 0 \\ 0 & -1 & 0 \\ 0 & 0 & 0 \\ 0 & 0 & 0 \end{bmatrix},$$

$$L_1^2 = \begin{bmatrix} 2 & 0 & 0 & 0 & -1 \\ 0 & 0 & 0 & 0 & 0 \\ 0 & 0 & 1 & -1 & 0 \\ 0 & 0 & -1 & 2 & 0 \\ -1 & 0 & 0 & 0 & 1 \end{bmatrix}$$

$$L_2^2 = \begin{bmatrix} -1 & 0 & 0 \\ 0 & 0 & 0 \\ 0 & 0 & 0 \\ 0 & 0 & -1 \\ 0 & 0 & 0 \end{bmatrix},$$

$$L_1^3 = \begin{bmatrix} 0 & 0 & 0 & 0 & 0 \\ 0 & 0 & 0 & 0 & 0 \\ 0 & 0 & 2 & -1 & 0 \\ 0 & 0 & -1 & 2 & -1 \\ 0 & 0 & 0 & -1 & 2 \end{bmatrix}$$

$$L_2^3 = \begin{bmatrix} 0 & 0 & 0 \\ 0 & 0 & 0 \\ 0 & -1 & 0 \\ 0 & 0 & 0 \\ 0 & 0 & -1 \end{bmatrix}.$$

The five eigenvalues of L_1^1 are denoted $\lambda_1 = 0, \lambda_2 = 0.328, \lambda_3 = 0.328, \lambda_4 = 2.618, \lambda_5 = 2.618$; The five eigenvalues of L_1^2 are denoted $\lambda_1 = 0, \lambda_2 = 0.328, \lambda_3 = 0.328, \lambda_4 = 2.618, \lambda_5 = 2.618$; The five eigenvalues of L_1^3 are denoted $\lambda_1 = 0, \lambda_2 = 0, \lambda_3 = 0.5858$, $\lambda_4 = 2, \lambda_5 = 3.4142$.$\zeta(1) \cup \zeta(2) \cup \zeta(3) = \{1, 2, 3, 4, 5\}$, this illustrates the result in Lemma 4.1. According to Lemma 4.2, the upper limit $\tau_{\min} = 0.46$ of the allowable delay of the designed system can be obtained.

Figs. 3 and 4 respectively show the state trajectories of the USSs at $\tau = 0.28, \tau_{\min} = 0.46, \tau = 0.47$, and $\tau = 0.55$. By comparison, according to the new control law designed by combining the joint connected switching topology and event-triggered control mechanism in this paper, when the time delay is 0.28 s, the state trajectory can quickly converge to the convex hull formed by the leader USS and maintain the equilibrium state during $0 \sim 0.25$ s.

In Fig. 3(b) and Fig. 4(f), when the communication delay increases to the maximum of 0.46 s, the state trajectories following USS can still recover stability within a limited time though they have obvious oscillations. In Fig. 3(c), when the communication delay increases to slightly exceed the maximum delay range $\tau = 0.47$, the state trajectory

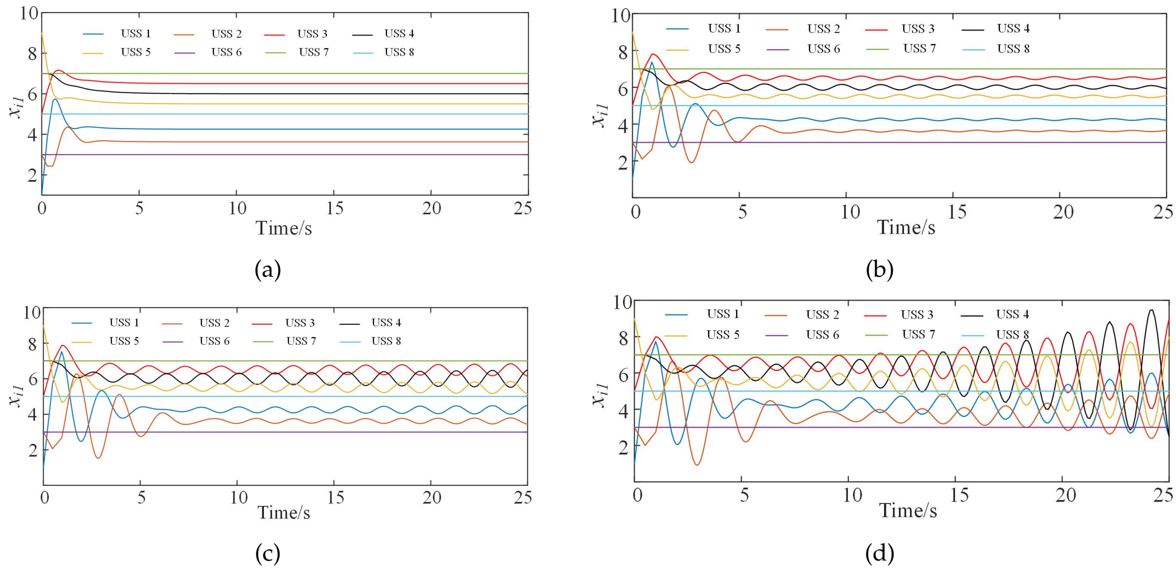

Fig. 3. (a), (b), (c), (d) are USS state trajectories $x_a(t)$ with delays of

$\tau = 0.28, \tau = 0.46, \tau = 0.47, \tau = 0.55$

following USS has relatively large oscillations and cannot keep moving in the minimum convex hull enclosed by the leader USS. In Fig. 3(d) and Fig. 4(h), since 0.55 s exceeds the given upper bound of communication delay, each state trajectory following USS cannot remain stable and converge to the convex hull formed by the leading USS.

Therefore, when the delay is within the range $(0, \tau_{\min})$, although the system will have topological switching, all the follower USS can gradually converge to the convex hull formed by the leader USS and eventually tend to be stable.

Figs. 5 and 6 show delay-free and $\tau = 0.46$ USSs following the trigger moment of the USS in the process of forming the containment control under the control protocol (11) and the event trigger condition (13), respectively. According to the simulation results, it can be verified that the system does not have Zeno behavior, and the smaller the delay, the lower the frequency of events triggered. Compared with continuous communication transmission, the proposed event-triggered control protocol can reduce the communication times of the system and save the energy resources of the system.

7. Conclusions

Articles on joint connected with a time delay switch topology conditions surrounded by USSs events trigger control problem is analyzed and the research, put forward a joint connected topology structure of the system communication constraints of smaller, on this basis, combining the situation of the communication time delay design surrounded by USSs control events trigger control rules, effectively reduce the communication load, reduce the energy consumption at the same time, It also makes the USSs more adaptable to the complex and changeable communication environment and can accomplish more complex tasks such as Marine dangerous goods handling, fire rescue, and cooperative transportation. The future work may consider the combination of bounding control and more complex nonlinear systems.

Acknowledgements

This work is supported by High Level Innovation Team and Outstanding Scholar Program of Guangxi Universities in 2018 "High-speed Railway Signal Vocational Education Equipment Technology R&d and Application" (Gui Jiaoren (2018) No. 35).

References

[1] Y. Liao, T. Du, and Q. Jiang, (2019) *"Model-free adaptive control method with variable forgetting factor for unmanned surface vehicle control"* **Applied Ocean Research** ***93***: 101945. DOI: 10.1016/j.apor.2019.101945.

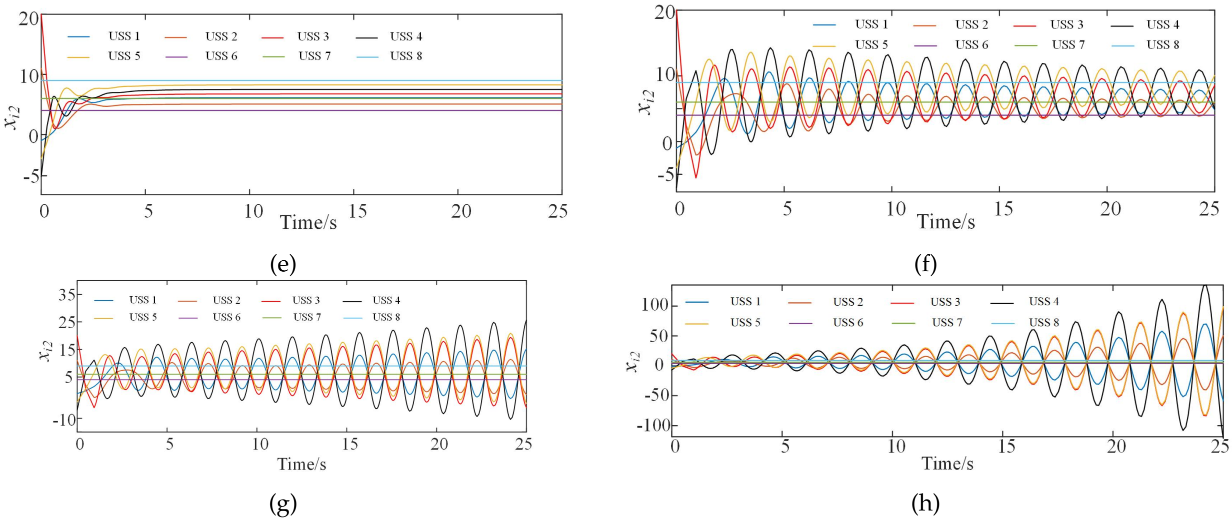

Fig. 4. (e), (f), (g), (h) are USS state trajectories $x_{i2}(t)$ with delays of

$\tau = 0.28, \tau = 0.46, \tau = 0.47, \tau = 0.55$

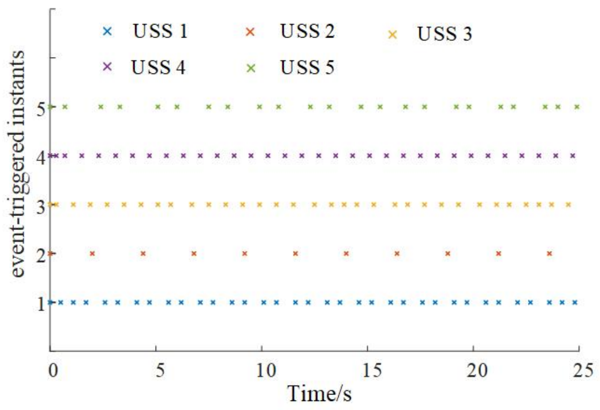

Fig. 5. Event-triggered instants without time-delay

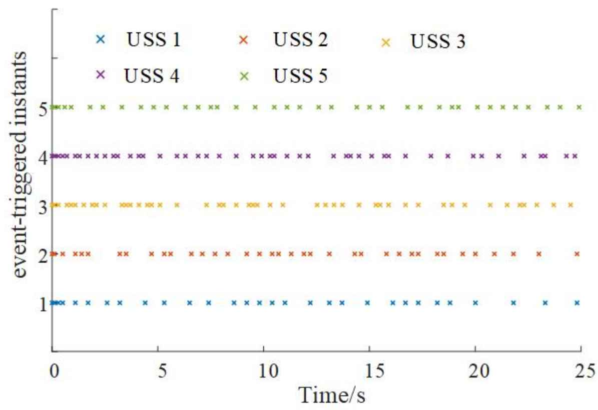

Fig. 6. Event-triggered instants with $\tau = 0.46$

[2] Z. Peng, J. Wang, D. Wang, and Q.-L. Han, (2020) *"An overview of recent advances in coordinated control of multiple autonomous surface vehicles"* **IEEE Transactions on Industrial Informatics *17***(2): 732–745. DOI: 10.1109/TII.2020.3004343.

[3] Z. Peng, D. Wang, T. Li, and M. Han, (2019) *"Output-feedback cooperative formation maneuvering of autonomous surface vehicles with connectivity preservation and collision avoidance"* **IEEE transactions on cybernetics *50***(6): 2527–2535. DOI: 10.1109/TCYB.2019.2914717.

[4] H. Qin, H. Chen, Y. Sun, and Z. Wu, (2019) *"The distributed adaptive finite-time chattering reduction containment control for multiple ocean bottom flying nodes"* **International Journal of Fuzzy Systems *21***: 607–619. DOI: 10.1007/s40815-018-0592-2.

[5] Y. Zou and Z. Meng, (2019) *"Coordinated trajectory tracking of multiple vertical take-off and landing UAVs"* **Automatica *99***: 33–40. DOI: 10.1016/j.automatica.2018.10.011.

[6] H. Yu, K. Meier, M. Argyle, and R. W. Beard, (2014) *"Cooperative path planning for target tracking in urban environments using unmanned air and ground vehicles"* **IEEE/ASME transactions on mechatronics *20***(2): 541–552. DOI: 10.1109/TMECH.2014.2301459.

[7] Y. Lan, G. Yan, and Z. Lin, (2010) *"Distributed control of cooperative target enclosing based on reachability and invariance analysis"* **Systems & Control Letters** ***59***(7): 381–389. DOI: 10.1016/j.sysconle.2010.04.003.

[8] K. Shojaei, (2015) *"Leader–follower formation control of underactuated autonomous marine surface vehicles with limited torque"* **Ocean Engineering** ***105***: 196–205. DOI: 10.1016/j.oceaneng.2015.06.026.

[9] X. Jin, (2016) *"Fault tolerant finite-time leader–follower formation control for autonomous surface vessels with LOS range and angle constraints"* **Automatica** ***68***: 228–236. DOI: 10.1016/j.automatica.2016.01.064.

[10] L. Liu, D. Wang, Z. Peng, C. P. Chen, and T. Li, (2018) *"Bounded neural network control for target tracking of underactuated autonomous surface vehicles in the presence of uncertain target dynamics"* **IEEE Transactions on Neural Networks and Learning Systems** ***30***(4): 1241–1249. DOI: 10.1109/TNNLS.2018.2868978.

[11] A. J. Sinisterra, M. R. Dhanak, and K. Von Ellenrieder, (2017) *"Stereovision-based target tracking system for USV operations"* **Ocean engineering** ***133***: 197–214. DOI: 10.1016/j.oceaneng.2017.01.024.

[12] T. I. Fossen. *Handbook of marine craft hydrodynamics and motion control*. John Wiley & Sons, 2011. DOI: 10.1002/9781119994138.

[13] H. Chen, J. Wang, C. Wang, J. Shan, and M. Xin, (2021) *"Distributed diffusion unscented Kalman filtering based on covariance intersection with intermittent measurements"* **Automatica** ***132***: 109769. DOI: 10.1016/j.automatica.2021.109769.

[14] L. Brinon-Arranz, A. Seuret, and A. Pascoal, (2019) *"Circular formation control for cooperative target tracking with limited information"* **Journal of the Franklin Institute** ***356***(4): 1771–1788. DOI: 10.1016/j.jfranklin.2018.12.011.

[15] J. X. L.-W. Kou, (2022) *"Target Fencing Control of Multiple Mobile Robots Using Output Feedback Linearization state under moving block system"* **Acta Automatica Sinica** ***48***(05): 1255–1291.

[16] J. X. L.-W. Kou S.-M. He, (2020) *"Square Root Cubature Kalman Filter-based Algorithm for Positioning Surface Ships"* **Shipbuilding of China** ***38***(3): 60–69.

[17] Y. Kao, C. Wang, H. R. Karimi, and R. Bi, (2014) *"Global stability of coupled Markovian switching reaction–diffusion systems on networks"* **Nonlinear Analysis: Hybrid Systems** ***13***: 61–73. DOI: 10.1016/j.nahs.2013.12.004.

[18] Y. Kang, D.-H. Zhai, G.-P. Liu, Y.-B. Zhao, and P. Zhao, (2014) *"Stability analysis of a class of hybrid stochastic retarded systems under asynchronous switching"* **IEEE Transactions on Automatic Control** ***59***(6): 1511–1523. DOI: 10.1109/TAC.2014.2305931.

[19] W. Ni and D. Cheng, (2010) *"Leader-following consensus of multi-agent systems under fixed and switching topologies"* **Systems & control letters** ***59***(3-4): 209–217. DOI: 10.1016/j.sysconle.2010.01.006.

[20] F. Wang, H. Yang, Z. Liu, and Z. Chen, (2017) *"Containment control of leader-following multi-agent systems with jointly-connected topologies and time-varying delays"* **Neurocomputing** ***260***: 341–348. DOI: 10.1016/j.neucom.2017.04.049.

[21] W. Liu, C. Yang, Y. Sun, and J. Qin, (2017) *"Observer-based event-triggered containment control of multi-agent systems with time delay"* **International Journal of Systems Science** ***48***(6): 1217–1225. DOI: 10.1080/00207721.2016.1249036.

[22] W. Zou and Z. Xiang, (2017) *"Event-triggered distributed containment control of heterogeneous linear multi-agent systems by an output regulation approach"* **International Journal of Systems Science** ***48***(10): 2041–2054. DOI: 10.1080/00207721.2017.1309595.

[23] W. Wei and J. Lv, (2018) *"Coordinated control of time-delayed multi-agent systems"*:

[24] Y.-n. Sun, W.-c. Zou, J. Guo, and Z.-r. Xiang, (2021) *"Containment control for heterogeneous nonlinear multi-agent systems under distributed event-triggered schemes"* **Frontiers of Information Technology & Electronic Engineering** ***22***(1): 107–119. DOI: 10.1631/FITEE.2000034.

[25] D. Wang, Z. Wang, Z. Wang, and W. Wang, (2020) *"Design of hybrid event-triggered containment controllers for homogeneous and heterogeneous multiagent systems"* **IEEE Transactions on Cybernetics** ***51***(10): 4885–4896. DOI: 10.1109/TCYB.2020.3007500.

[26] S. Boyd, L. El Ghaoui, E. Feron, and V. Balakrishnan. *Linear matrix inequalities in system and control theory*. SIAM, 1994.